HHS Public Access

Author manuscript

Circ Cardiovasc Genet. Author manuscript; available in PMC 2016 June 01.

Published in final edited form as:

Circ Cardiovasc Genet. 2015 June ; 8(3): 516–528. doi:10.1161/CIRCGENETICS.114.000921.

Non-biased molecular screening identifies novel molecular regulators of fibrogenic and proliferative signaling in myxomatous mitral valve disease

Nassir M. Thalji, MBChB[1,*], **Michael A. Hagler, BS**[1,*], **Heyu Zhang, MD, PhD**[1], **Grace Casaclang-Verzosa, MD**[1], **Asha A. Nair, MS**[2], **Rakesh M. Suri, MD, DPhil**[1], and **Jordan D. Miller, PhD**[1,3]

[1]Division of Cardiovascular Surgery, Mayo Clinic, Rochester, Minnesota

[2]Department of Biomedical Statistics and Informatics, Mayo Clinic, Rochester, Minnesota

[3]Department of Physiology and Biomedical Engineering, Mayo Clinic, Rochester, Minnesota

Abstract

Background—Pathological processes underlying myxomatous mitral valve degeneration (MMVD) remain poorly understood. We sought to identify novel mechanisms contributing to development of this condition.

Methods and Results—Microarrays were used to measure gene expression in 11 myxomatous and 11 non-myxomatous human mitral valves. Differential gene expression (thresholds $p<0.05$; fold-change>1.5) and pathway activation (Ingenuity) were confirmed using qRT-PCR and immunohistochemistry. Contributions of BMP4 and TGF-β2 to differential gene expression were evaluated *in vitro*. Contributions of angiotensin-II to differential pathway activation were examined in mice *in vivo*. 2,602 genes were differentially expressed between myxomatous and non-myxomatous valves. Canonical TGF-β signaling was increased in MMVD due to increased ligand expression and de-repression of SMAD2/3 signaling and was confirmed with qRT-PCR and immunohistochemistry. Myxomatous valves demonstrated activation of canonical BMP and Wnt/β-catenin signaling and upregulation of their common target Runx2. Our dataset provided transcriptional and immunohistochemical evidence for activated immune cell infiltration. *In vitro* treatment of mitral valve interstitial cells with TGF-β2 increased β-catenin signaling at mRNA and protein levels, suggesting interactions between TGF-β2 and Wnt signaling. *In vivo* infusion of mice with angiotensin-II recaptured several changes in signaling pathways characteristic of human MMVD.

Conclusion—These data support a new disease framework whereby activation of TGF-β2, BMP4, Wnt/β-catenin, or immune signaling play major roles in the pathogenesis of MMVD. We propose these pathways act in a context-dependent manner to drive phenotypic changes that

Address for Correspondence: Jordan D. Miller, PhD, Division of Cardiovascular Surgery, Mayo Clinic College of Medicine; 200 First Street SW, Rochester, Minnesota 55905, United States. Phone: (507) 255-7621; Fax: (507) 255-7378; miller.jordan@mayo.edu or Rakesh M. Suri, MD, DPhil, Division of Cardiovascular Surgery, Mayo Clinic College of Medicine; 200 First Street SW, Rochester, Minnesota 55905, United States. Phone: (507) 255-7067; Fax: (507) 255-7378; suri.rakesh@mayo.edu.

*These authors contributed equally to this work.

Disclosures: None

fundamentally differ from those observed in aortic valve disease, and open novel avenues guiding future research into the pathogenesis of MMVD.

Keywords

Mitral valve; Surgery; Pathology; Molecular biology

INTRODUCTION

Myxomatous mitral valve degeneration (MMVD) has an estimated prevalence of 2–3% in the general population[1]. Abnormal thickening of valve leaflets alongside thickening, thinning or elongation of the chordae tendinae are hallmark features of MMVD[2,3]. The resultant disruption of the structural integrity of the valvular apparatus leads to the eventual development of mitral valve prolapse (MVP). In the absence of appropriate and timely intervention, MVP secondary to MMVD sequentially progresses to mitral regurgitation, impaired left ventricular (LV) function and heart failure, and ultimately death[1,4].

Surgical strategies remain the therapeutic gold standard in MMVD[5], and normal life expectancy can be restored following mitral valve repair [6–8]. Molecular mechanisms contributing to MMVD remain poorly understood, however, and have been largely confined to the role of transforming growth factor-beta 1 (TGF-β1). Upregulation of TGF-β1 has been reported in animals [9,10] and humans with MVP[11,12], and is thought to contribute to extracellular matrix remodeling and fibrosis [12,13]. Interestingly, hypertension is a major risk factor for accelerated progression of MMVD[14], and a recent report implicated angiotensin II (AngII) in the activation of TGF-β signaling in valvular interstitial cells *in vitro*[11]. To date, however, identification of alternative and/or parallel pathways outside of TGF-β1 signaling that contribute to initiation or progression of MMVD have been limited.

To address this issue, we used comprehensive whole genome expression arrays as a non-biased method to identify novel signaling pathways altered in myxomatous versus non-myxomatous human mitral valves. To validate the relative importance and contribution of some of the identified pathways in the development of MMVD, we performed directed *in vitro* experiments in human/mouse mitral valve interstitial cells (MVICs), as well as the molecular and phenotypic consequences of *in vivo* AngII infusion in murine mitral valve tissue. Our overriding goals were to identify novel mechanisms contributing to development of MMVD and to determine the extent to which an experimental mouse model can recapture molecular and/or phenotypic aberrations characteristics of MMVD.

METHODS

Non-Biased Identification of Novel Signaling Pathways in MMVD

Affymetrix Human Genome U133 Plus 2.0 expression arrays were used to measure differential gene expression in a random sample of 11 myxomatous and 11 non-myxomatous human mitral valves obtained during surgeries at Mayo Clinic in Rochester, MN (see supplement for details). Mayo Clinic's Institutional Review Board approved the current study, and valid informed consent was obtained for all patients.

Confirmation of Differentially Regulated Signaling Pathways in MMVD

Differential expression of key pathway genes between myxomatous and non-myxomatous human mitral valves was confirmed by quantitative real-time PCR (qRT-PCR) (see Table S1 for gene expression primers used) and immunohistochemistry (see supplement for details).

In Vitro Model of MMVD

Human and murine (C57BL/6J) MVICs were harvested and cultured, and subsequently treated with exogenous bone morphogenetic protein 4 (BMP4), TGF-β2 or control saline for 24h. Consequent molecular changes were identified using qRT-PCR, western blotting, and immunocytochemistry (see supplement for details).

In Vivo Model of MMVD

Young C57BL/6J mice (2–3 months of age) were treated with pressor doses of angiotensin II (AngII) or saline via osmotic minipump for 14 days. Molecular changes in mitral valves were assessed by qRT-PCR and immunohistochemistry. Echocardiography was used to assess mitral valve and LV function on day 14 post-minipump implantation (see supplement for details). All protocols pertaining to animal studies were approved by the Mayo Clinic Institutional Animal Care and Use Committee and conformed to guidelines set forth by the National Institutes of Health and the Guide for the Care and Use of Laboratory Animals.

Statistical Analyses

Differential gene expression between myxomatous and non-myxomatous mitral valves was determined by linear modeling using t-test, with significance thresholds of a 1.5 fold-change in expression and a p-value <0.05. Secondary analysis adjusting for multiple comparisons was carried out using the false discovery rate (FDR) statistical approach. Adjusted p-values (q-values) were obtained and two commonly used significance thresholds of $q<0.05$ and $q<0.1$ were applied. Ingenuity Pathway Analysis systems were used to identify differentially regulated signaling pathways (Ingenuity Systems Inc.).

Results of confirmatory qRT-PCR and immunohistochemical staining were compared between myxomatous and non-myxomatous human mitral valves using student's *t*-test. Linear regression and coefficients of determination (R^2) were used to depict correlations between microarray and qRT-PCR-determined gene expression for all validated genes (Table S2).

Differential gene expression (qRT-PCR) and protein levels (immunohistochemistry) between *in vivo* saline versus AngII treated mouse mitral valves were compared using student's *t*-tests. Results of qRT-PCR and western blotting experiments comparing effects of *in vitro* treatment with TGF-β2 or BMP4 to control conditions (saline/vehicle) were analyzed using Dunnett's test for multiple comparisons. Significance thresholds of $p<0.05$ were used throughout. For further details, see expanded statistical methods in the manuscript supplement.

RESULTS

Differential Gene Expression in MMVD

Patient-specific data including demographics, surgical indication and baseline medications are outlined in tables S3–5. From our primary microarray analyses, 2,602 unique genes were differentially expressed between myxomatous and non-myxomatous human mitral valves (1,454 up-regulated, 1,148 down-regulated) (Figure S1, Table S6). From our secondary microarray analyses, 2,125 unique genes were differentially expressed between myxomatous and non-myxomatous human mitral valves (1,317 up-regulated, 808 down-regulated) with a significance threshold of $q<0.05$. When using a significance threshold of $q<0.1$, all 2,602 genes from our primary analysis retained statistical significance (q-values in Table S6). Since Ingenuity Pathway Analyses using significance thresholds of $q<0.05$ and $q<0.1$ yielded near identical results for key differentially regulated signaling cascades, the subsequent data present herein are derived from the primary analysis dataset.

TGF-β Signaling and Gene Expression are Increased in MMVD

Microarray pathway analyses identified significantly dysregulated expression of genes associated with canonical TGF-β signaling in myxomatous mitral valves (Figure 1A). More precisely, TGF-β2 ligand, intra-nuclear transcription factors (Runt-related transcription factor 2 [Runx2]), co-activators (Cyclic-AMP-responsive element-binding protein 5 [CREB5]), and pro-fibrotic gene products (Collagen type I, alpha I [COL1A1], matrix metalloproteinases [MMP] 2 and 16, Fibroblast activation protein [FAP], Fibronectin (FN1), and Fascin [FSCN1]) were also increased in myxomatous valves. Expression of the decoy receptor BAMBI (BMP and activin membrane-bound inhibitor homolog [Xenopus laevis]), intracellular inhibitors of TGF-β signaling (Salt-inducible kinase 1 [SIK1]) and transcriptional repressors (c-Myc, TGF-β-induced factor [TGIF]) were reduced in myxomatous tissue. qRT-PCR confirmed significant changes in TGF-β2 ligand (Figure 1B), BAMBI (Figure 1C), and SIK1 (Figure 1D) (all $p<0.05$). Figure 1E depicts a working model of these changes in the context of canonical TGF-β signaling.

Multiple Classically “Osteogenic” Signaling Pathways are Increased in MMVD

Increased BMP signaling in myxomatous mitral tissue was evident from the microarray screen (Figure 2A), as expression of BMP4, transcriptional co-activators (CREB5) and BMP target genes (Runx2, Wnt-inducible pathway protein 1 [WISP1]) was increased in myxomatous valves. In contrast, intracellular signaling inhibitors (transducer of erbB2 [TOB2]) and transcriptional co-repressors (c-Myc, TGIF) were reduced in diseased mitral valves. qRT-PCR confirmed changes in BMP4 ligand (Figure 2B) and Runx2 (Figure 2C) in myxomatous versus non-myxomatous tissue (both $p<0.05$). Immunohistochemical staining demonstrated increases in the canonical intracellular signaling protein pSMAD1/5/8 (SMA mothers against decapentaplegic) (Figures 2D–E, S2A). Figure 2F outlines a working model for contributions of these changes towards BMP signaling.

Microarray pathway analyses also suggested that canonical Wnt/β-catenin signaling was increased in valve tissue from patients with MMVD (Figure 3A). Levels of Wnt ligand (Wnt9A) and receptor (Frizzled 8 [FZD8]), extracellular positive modulators of Wnt

signaling (R-Spondin 2 [RSPO2], Norrie disease (pseudoglioma) [NDP]), intranuclear transcription factors (Transcription factor 4 [TCF4]), and classically "pro-calcific" gene products (Runx2, WISP1) were increased in MMVD. In contrast, transcription repressors (HMG-box transcription factor 1 [HBP1]) and co-repressors (Transducer-like enhancer of split 1 [TLE1]) were reduced in MMVD. qRT-PCR confirmed increases in Wnt9A, FZD8, RSPO2, and WISP1 (Figures 3B–E; all $p<0.05$). Figure 3F delineates a model representation of these changes in relation to Wnt signaling.

Evidence of Immune Cell Infiltration and Activation in Myxomatous Mitral Valves

There was evidence of immune cell infiltration and activation in myxomatous versus non-myxomatous mitral valve tissue (Figure 4A). Cell-surface receptors CD14 and CD83 alongside cytokines (Interleukin-7 [IL-7], Chemokine (C-X3-C motif) ligand 1 [CX3CL1]) and cytokine receptors (Chemokine (C-X3-C motif) receptor 1 [CX3CR1]) were increased in MMVD. Levels of toll-like receptors (TLRs) 3 and 7 were also increased in myxomatous tissue. Upregulation of CD14, CD83 and CX3CR1 in myxomatous valves was corroborated by qRT-PCR (Figures 4B–D; all $p<0.05$). Immunohistochemical staining for anti-CD14 antibodies additionally verified abnormally increased infiltration of immune cells in myxomatous valves (Figures 4E, S12B). Immune localization in mitral tissue appeared independent of IL-6 – a cytokine commonly used as a marker of inflammation – which had an approximately 17-fold reduction in expression in myxomatous valves (Figure 4A, see full microarray dataset in supplement). Figure 4F depicts a working model for these transcriptional changes as relating to immune activation and infiltration.

Evidence of Increased Cellular Proliferation in MMVD

From the microarray dataset, we identified reduced expression of the cell-cycle inhibitor CDKN1A (see full microarray dataset in supplement) in myxomatous valves, confirmed by qRT-PCR (Figure S3A). Reciprocally, we used immunohistochemistry to demonstrate up-regulation of the proliferation marker proliferation cell nuclear antigen (PCNA) in myxomatous valves (Figure S2C–D, S3B–C).

Molecular Cross-Talk in MMVD

Figure 5 depicts the network of potential protein-protein interactions between molecules differentially expressed in myxomatous versus non-myxomatous human mitral valves, and their neighboring interactors, derived using PathwayLinker [15]. The specific goal of this figure is to highlight numerous interactions between key molecules that were identified as differentially regulated in our microarray analysis (i.e. TGF-β signaling, BMP signaling, Wnt/β-catenin signaling, immune-related processes), and thereby provide an initial framework to guide future investigation into complex molecular interactions contributing to the pathogenesis of MMVD.

Effects of In Vitro Treatment with Exogenous TGF-β2 and BMP4 on Pro-fibrotic, "Pro-Calcific", and Immune-related Signaling Responses in Non-Myxomatous MVICs

TGF-β2 treatment increased protein levels of pSMAD2 on western blot analysis (Figures 6A, S4A) though immunocytochemical changes failed to show significant differences

(Figures 6B, S5A). TGF-β2 increased mRNA levels of the fibrogenic target gene COL1A1 (Figure 6C), and expression of intracellular TGF-β signaling inhibitors SIK1 (Figure 6D), SMAD specific E3 ubiquitin ligase (SMURF) 1 and SMURF2 (Figure S6A–B) in human MVICs. Exogenous treatment of human MVICs with TGF-β2 yielded significant reductions in expression of the decoy receptor BAMBI (Figure S6C). Conversely, following BMP4 treatment, BAMBI expression was increased (Figure S6C) in the absence of other visible alterations in TGF-β signaling (Figures 6A–D). With the exception of unchanged BAMBI expression following BMP4 treatment, similar changes were observed in murine MVICs (Figure S7–S9, S10A).

Considering BMP-network genes, *in vitro* TGF-β2 treatment did not significantly alter pSMAD1/5/8 protein levels (Figures 6E–F, S4B, S5B) or Runx2 expression (Figure 6G), despite reducing mRNA levels of BMP4 (Figure 6H). Protein levels of pSMAD1/5/8 were increased following exogenous BMP4 treatment (Figures 6E–F), although Runx2 mRNA appeared unchanged (Figure 6G), and BMP4 expression was again reduced (Figure 6H). Similar changes were observed in murine MVICs (Figures S7, S8B, S10B).

Although total protein levels of β-catenin (Figure 6I, Figure S4C) were unaltered following exogenous TGF-β2, immunocytochemical analysis revealed increased nuclear translocation of β-catenin (Figures 6J, S5C). This coincided with increased mRNA levels of both the Wnt-target gene WISP1 (Figure 6K) and ligand Wnt9A (Figure 6L). In contrast, BMP4 treatment did not impact levels or expression of Wnt-pathway proteins and genes, respectively (Figures 6I–L). Similar changes were observed in murine MVICs (Figures S7, S8C, S10C).

Although protein levels of CD14 were unchanged (Figures 6M–N, S5D), *in vitro* treatment with TGF-β2 and BMP4 separately reduced mRNA levels of CD14 (Figure 6O), while TGF-β2 treatment induced a significant increase in CD83 expression in human MVICs (Figure 6P). Similar changes were observed in murine MVICs (Figure S7).

In Vivo Treatment with AngII Partially Recaptures Molecular and Phenotypic Features of Human MMVD in Murine Mitral Valves

The mean change in systolic blood pressure between baseline readings and Day 14 post-minipump implantation was an increase of 61 ± 3 mmHg versus an increase of 6 ± 3 mmHg in AngII and Saline infused mice, respectively ($p < 0.05$). Following 14 days of AngII treatment via minipumps, immunochemical staining with pSMAD2 was significantly increased (Figures 7A, S11A, S12A). Coincident with this, mRNA levels of fibrogenic genes, CTGF and MMP2 (Figures 7B–C), and TGF-β2 ligand (Figure 7D) were increased following AngII infusion, whereas expression of the decoy receptor BAMBI was decreased (Figure 7E).

While staining for pSMAD1/5/8 appeared unchanged in AngII versus saline infused mice (Figures 7F, S11B, S12B), expression of classically pro-osteogenic genes MSX2 and Runx2 were significantly increased (Figures 7G–H); in the absence of altered expression of BMP4 and the intracellular BMP-pathway inhibitor TOB2 (Figures 7I–J).

Furthermore, AngII infusion was associated with increased staining for β-catenin in murine mitral valves (Figures 7K, S11C, S12C). This corresponded with increased expression of the Wnt target gene, WISP1 (Figure 7L), and decreased expression of the Wnt signaling inhibitor, Axin2 (Figure 7M), despite the absence of change in mRNA levels of Wnt9A ligand or the Wnt-receptor FZD8 (Figures 7N–O).

Although AngII infusion did not alter expression of the cytokine IL-7 (Figure 7P) or pattern-recognition receptors CD14 and CD83 (Figure 7Q–R), it did induce increased mRNA levels of the immune receptor TLR7 (Figure 9S). Furthermore, AngII infusion was associated with increased cellular proliferation in murine mitral valves, as evidenced by increased Ki-67 staining (Figures S11D–E, S12D–E)

To exclude the possibility of myocardial contamination of mitral valve tissue, the cardiomyocyte-specific proteins MyH6 and Myl2 were measured in valve leaflets and ventricular tissue. Expression of both genes was dramatically higher in ventricular tissue compared to leaflet tissue, and there were no differences between saline or AngII-treated groups within each tissue type (see supplementary figure S13).

Finally, in the absence of a difference in ejection fraction (Figure 7T), LV mass (Figure 7U), LV end-systolic dimension (Figure S14A) or LV end-diastolic dimension (Figure S14B) between AngII and saline-infused mice, echocardiographic assessment on day 14 post-minipump implantation revealed evidence of trace mitral regurgitation in approximately 63% (5/8) of AngII-treated (Figure 7V) versus 38% (3/8) of saline-infused mice (Figure 7W) (p=NS).

DISCUSSION

Using a non-biased, high-throughput approach to molecular characterization, this study elucidates several novel molecular mechanisms that may underlie progression of MMVD to mitral valve prolapse. The key findings of our microarray analysis are: 1) TGF-β signaling is increased in myxomatous mitral valve tissue due to increased ligand expression and de-repression of canonical SMAD2/3 signaling, 2) canonical BMP and Wnt/β-catenin signaling pathways are increased in MMVD, 3) TGF-β, BMP and Wnt/β-catenin pathways in MMVD are associated with matrix remodeling, “pro-calcific” and pro-proliferative cellular processes, and 4) activated immune cells are localized to myxomatous mitral valves in a manner independent of a “classic” inflammatory immune response. Our subsequent *in* vitro and *in vivo* experiments suggest: 1) up-regulation of TGF-β signaling in MMVD may serve to trans-activate Wnt/β-catenin signaling and 2) AngII signaling *in vivo* is sufficient to activate some—but not all—differentially activated signaling cascades observed in human MMVD.

Transforming Growth Factor-β Signaling is De-Repressed in MMVD

A novel finding of this study is that induction of TGF-β signaling in MMVD is due not only to increased ligand expression, but also increases in multiple molecules that facilitate transduction of canonical TGF-β signaling. Our finding that TGF-β2 is increased in MMVD is consistent with prior reports of increased TGF-β ligand expression in animal models of

MVP and human MMVD[9–12]. We also uncovered increased levels of the adaptor molecule Disabled2 (DAB2, which has been shown to amplify canonical TGF-β signaling by recruiting receptor-activated SMADs2/3 to TGF-β receptor[16]), the transcriptional co-activator CREB5 and numerous TGF-β/SMAD2/3 target genes.

A major novel finding of this study, however, is that levels of the TGF-β decoy receptor, BAMBI[17], and the TGF-β signaling inhibitor SIK1[18] – which may synergize with the inhibitory SMAD7 – were reduced in MMVD. Furthermore, expression of the transcriptional co-repressors c-Myc[19] and TGIF[20] were also down-regulated in MMVD. Importantly, while these molecular aberrations support current working models in which excessive TGF-β signaling may culminate in matrix remodeling and tissue fibrosis in MMVD, specifically they suggest that this phenomenon may in part be mediated by de-repression of canonical signaling pathways.

Bone Morphogenetic Protein Signaling is Activated in MMVD

Our current data also demonstrate robust activation of BMP signaling in MMVD. While members of the BMP family are implicated in the pathogenesis of cardiovascular calcification [21], the role of BMP signaling in mitral valve prolapse – a phenotypically distinct disease entity not typically associated with leaflet calcification or aging – is yet to be clearly elucidated.

Consistent with one previous study [22], we found increases in BMP4 in myxomatous valves, and – to our knowledge – for the first time demonstrate that activation of this pathway is via canonical pSmad1/5/8 signaling. Similar to TGF-β signaling, BAMBI, SIK1, and TOB2—also negative regulators of canonical BMP signaling—were also reduced in myxomatous mitral valves. Critically, these data again support a novel disease model whereby de-repression of TGFβ superfamily signaling is integral in the pathogenesis of MMVD.

Wnt/β-catenin signaling is activated in MMVD

To our knowledge, this study is the first to demonstrate activation of canonical Wnt signaling pathways in human MMVD. To be precise, expression of Wnt9A, Wnt-receptor FZD8 and classic Wnt-target genes (WISP1 and Runx2) were increased in myxomatous valves [23]. Interestingly, we also uncovered increases in RSPO2, which can increase Wnt signaling through attenuation of DKK1-dependent inhibition of Wnt ligands[24,25]

While previous work described Wnt pathway-dependent induction of cellular proliferation in valvular interstitial cells *in vitro*[26], we believe our data are the first to suggest that this phenomenon may be mediated by the Wnt ligand Wnt9A, and the Wnt-target gene Runx2. Recently, Runx2 has been shown to mediate cellular proliferation through repression of CDKN1A – mRNA levels of which are reduced in our microarray – and may thus play multiple, context-dependent roles in the development of MMVD[27–29]. While upregulation of Runx2 in myxomatous human mitral valves has been reported in one previous study, this has been predominantly discussed in the context of cell lineage determination (i.e., promotion of chondrogenesis), and compared to the molecular changes seen in calcific aortic

valve stenosis[30]. Importantly, however, leaflet and/or annular calcification are not hallmarks of MMVD.

Abnormal Immune Infiltration in MMVD

To our knowledge, these data are the first to demonstrate robust evidence of immune cell infiltration in MMVD. In the present study, we found increases in the pattern recognition receptors CD14 and CD83 in myxomatous valves, suggestive of localization of immature and mature antigen presenting cells (APC) [31,32], respectively. We propose that future studies aimed at understanding interactions between IL-7, CX3CL1, CX3CR1, and immune cell infiltration, may identify a maladaptive "wound repair" response in MMVD involving TGF-β, valvular interstitial cell activation, extracellular matrix remodeling, and functional leaflet prolapse[33,34].

TGF-β2 and BMP4: Activation and Cross-Talk *In Vitro*

Through treatment of non-myxomatous cultured MVICs with recombinant TGF-β2 and BMP4 we aimed to glean further insight into the relationship between and interplay amongst the various dysregulated signaling pathways identified by our microarray analysis.

Apart from increasing protein levels of pSMAD1/5/8, treatment of MVICs with exogenous BMP4 did not trigger robust increases in osteogenic gene expression, but did increase expression of negative regulators of BMP signaling (e.g. BAMBI). Exogenous BMP4 also did not appear to transactivate canonical TGF-β or Wnt/β-catenin signaling cascades. While this may be in part a function of treatment duration[22], our data collectively leave the precise contribution of BMP4 signaling in MMVD rather enigmatic.

As expected, *in vitro* TGF-β2 treatment induced canonical SMAD2 signaling and expression of multiple pro-fibrotic genes. Our finding of increased expression of intracellular inhibitors of SMAD2/3 signaling (e.g. SIK1, SMURF1, SMURF2) is in keeping with a negative feedback loop that would be expected following short-term TGF-β2 treatment. Interestingly, however, we found reduced expression of the decoy receptor BAMBI following TGF-β2 treatment, consistent with a paradoxical picture of a positive feedback loop. This finding suggests that TGF-β2-induced reductions in BAMBI in humans with MMVD may serve to further de-repress and potentiate BMP and TGF-β signaling cascades.

Of equal significance is our finding that TGF-β2-treated MVICs demonstrate enhanced expression of Wnt9A and the classic Wnt-target gene WISP1. When considered in conjunction with the immunocytochemical evidence of increased nuclear β-catenin that suggests induction of canonical Wnt signaling – and despite unchanged total β-catenin – we propose that aberrant TGF-β activation may function to activate – or potentially transactivate – canonical Wnt/β-catenin signaling in MMVD. This is in keeping with prior evidence suggesting a key interaction between TGF-β and Wnt signaling pathways in promoting fibrosis in other tissues[35].

Previous data have shown that TGF-β and BMP signaling are also capable of inducing transcription of Runx2, as well as promoting its activity as a transcription factor [36]. While our cell culture data do not conclusively support convergence of these signaling pathways on

induction of Runx2 in mitral valve interstitial cells, *in vitro* effects of TGF-β superfamily ligands are highly context-dependent (e.g., concentration, duration, etc.), and thus future studies are required to precisely characterize the contributions of TGF-β, BMP and Wnt/β-catenin signaling to the transcriptional patterns observed in myxomatous valves.

TGF-β2 and BMP4: Interactions With Immune Signaling In Vitro

In the current study, treatment of human MVICS with either BMP4 or TGF-β2 resulted in significant reductions in the immature APC marker CD14. In contrast, treatment of cells with TGF-β2 resulted in small but significant increases in expression of CD83, a robust marker of mature APCs. While the functional consequences of these changes remain unclear, our understanding of the function of the immune system in the pathogenesis of MMVD is likely to be a critical future area of investigation.

AngII as a Common Link in MMVD?

While hypertension is a long-standing risk factor for progression of MMVD to severe prolapse[14], angiotensin Type I receptor activation has only recently been directly implicated in TGF-β-induced fibrogenic signaling in MVICs *in vitro*[11]. In this study, treatment of mice with AngII induced robust activation of canonical SMAD-dependent TGF-β2 signaling and target gene expression. While this observation is consistent with prior reports of AngII-mediated activation of TGF-β signaling in myocardial tissue[37], our work extends these findings by demonstrating that *in vivo* AngII can significantly reduce expression of the decoy receptor BAMBI in murine mitral valves. These findings broach the intriguing possibility that AngII-induced canonical TGF-β signaling may be potentiated by de-repression at multiple points in this cascade.

Our observation that Wnt/β-catenin signaling is increased in AngII-infused mice is intriguing given emerging data that some of the transcriptional consequences of TGF-β receptor activation occur via activation (or trans-activation) of canonical Wnt/β-catenin signaling. This is supported by our finding of increased expression of the Wnt-target gene WISP1 in AngII-treated mice. Critically, we also found that AngII-mediated increases in Runx2 are associated with upregulation of the cell proliferation marker Ki-67, which is consistent with our working hypothesis that Runx2 does not drive overt calcification in MMVD but instead promotes cellular proliferation. We propose that future investigation into interactions between TGF-β, Wnt/β-catenin, Runx2, and cell-cycle checkpoint proteins will lend key insights into the pathogenesis of MMVD.

Notably, AngII infusion did not recapture changes in BMP and Wnt ligands, or immune cell markers that we observed in human MMVD. AngII was similarly unable to induce a consistent and robust phenotype of prolapse and regurgitation in murine mitral valves. These findings suggest that two weeks of AngII-induced hypertension, at least in isolation, is insufficient to account for the entire fingerprint of human MMVD. Furthermore, this should incite caution before it is suggested that MMVD is simply an AngII-mediated disease or that monotherapy aimed at the Renin Angiotensin System would be a sufficient therapeutic strategy to slow progression of MMVD[11].

Despite these drawbacks, we believe these data suggest that administration of AngII in mice may have some utility in the evaluation and dissection of very specific signaling cascades (e.g. TGF-β and Wnt/β-catenin signaling) observed in MMVD using pharmacological interventions and/or genetically modified animals.

Complex Molecular Interactions in MMVD

Our microarray analyses provide evidence in support of the contribution of TGF-β, BMP, Wnt/β-catenin and immune pathways in the pathogenesis of MMVD. However, the potential interactions and cross-talk between these pathways and their component genes/proteins are likely to be far more complex (Figure 5), and future experimental and interventional studies are required to more clearly elucidate the precise relationship between these signaling cascades. Importantly, understanding mechanisms mediating the recurrent and apparently widespread phenomenon of transcriptional derepression of pathological signaling cascades will be essential to the development of novel therapeutic interventions aimed at slowing progression of MMVD.

Study Limitations—Human Data

Several limitations of the current study warrant discussion. First, the limited amount of tissue available from human subjects meant it was not feasible to validate altered expression of all genes identified from microarray screens using RT-PCR. We therefore focused confirmatory analyses on key genes that would support evidence of canonical signaling pathway activation.

Second, although the human control valves obtained from transplant patients' hearts were morphologically normal in appearance, they were likely exposed to undue stress and thus are not truly "normal". Importantly, however, these valves were non-myxomatous and historically have been deemed the best available controls for this line of investigation.

Although the majority of human valves studied were from males, cluster pattern analysis of high-throughput gene expression data did not identify any apparent sex differences between sexes. Furthermore, difficulty in acquiring age-matched samples of non-myxomatous and myxomatous mitral tissue for study resulted in discrepant mean ages between the two groups. There were not, however, correlations between age and gene expression amongst any qRT-PCR-validated genes. Nevertheless, there are multiple plausible mechanisms that could contribute to differences in the biology and/or natural history of mitral valve disease with aging, across sexes, and when accounting for environmental stressors (e.g. smoking), making these important areas for future investigation.

Statistically, a potential limitation of our primary statistical analysis was that we did not adjust for multiple comparisons in order to cast a "broad net" that would allow us to identify novel genes and pathways contributing to the development and/or progression of MMVD. After conducting a secondary, more stringent analysis of the data that adjusted for multiple comparisons ($q<0.05$), we found robust conservation of the vast majority of genes that were differentially regulated in our dataset, and more than 90% of signaling cascades identified by Ingenuity Pathway Analyses remained significantly differentially regulated between myxomatous and non-myxomatous cohorts. Most importantly, TGF-β, BMP, Wnt/β-catenin

and immune signaling genes featured heavily and repeatedly in the most differentially-regulated signaling cascades and did not change the interpretation of our results. Altogether, we believe the presentation and focus on our primary analyses is in line with our goal of identifying a broad array of novel molecules and signaling cascades whose mechanistic role in MMVD can be interrogated using experimental models of MMVD in the future.

Finally, we acknowledge that our working model and proposed molecular contributors to MMVD have not been fully and mechanistically validated herein. Our cell culture experiments predominantly serve to highlight the exploratory and hypothesis-generating nature of the current manuscript, and extensive *in vitro* studies are warranted to validate the roles of these pathways in MMVD.

Study Limitations—Mouse Data

One limitation of our *in vivo* animal studies that the molecular changes observed in AngII treated animals may have been a consequence of hypertensive forces on the valve rather than AngII *per se*. While our experimental design did not specifically address this, previous studies demonstrated that AngII is capable of driving deleterious molecular and phenotypic changes in cardiovascular tissues (including TGF-β expression, immune cell recruitment, fibroblast activation, etc.) independent of changes in blood pressure[38–40]. Future studies focused on understanding the interactions between AngII and blood pressure will provide critical insights into the pathogenesis of MMVD.

We also acknowledge that treatment of mice with AngII for two weeks represents a relatively short period of time. While longer durations of treatment may augment the magnitude of molecular and phenotypic changes in mitral valves, such experiments are frequently associated with formation of aortic aneurysms or development of aortic valve regurgitation. Thus, future studies focused on treatment for longer durations will require development of protocols that do not confound data interpretation due to “off target”/ confounding changes in cardiovascular function or attrition of animals from AngII-treated groups.

CONCLUSIONS

Collectively, these data provide evidence in support of a new disease framework in myxomatous mitral valve disease, whereby fibrogenic, “osteogenic”, and proliferative signaling are robustly activated in myxomatous valve tissue, and de-repression of these signaling cascades may be a key permissive mechanism promoting disease progression. While some of these changes appear reminiscent of the molecular signature present in calcific aortic valve disease, it is critical to note that the phenotypic consequences of these changes are dramatically different and are likely to act in a highly context-dependent manner. Furthermore, these signaling pathways may be subject to initiation and/or modulation by the immune system. Ultimately, we believe that these findings open up numerous novel areas of research that may lead to non-surgical therapies to slow progression of MMVD.

Supplementary Material

Refer to Web version on PubMed Central for supplementary material.

Acknowledgments

Funding Sources: This work was supported by HL092235 (JDM), HL111121 (JDM), UL1TR000135 (Institutional Clinical and Translational Science Award), the Robert and Arlene Kogod Center on Aging at Mayo Clinic, and the Mayo Clinic Center for Regenerative Medicine.

References

1. Freed LA, Levy D, Levine RA, Larson MG, Evans JC, Fuller DL, et al. Prevalence and Clinical Outcome of Mitral Valve Prolapse. N Engl J Med. 1999; 341:1–7. [PubMed: 10387935]
2. Guthrie RB, Edwards JE. Pathology of the Myxomatous Mitral Valve: Nature, Secondary Changes and Complications. Minn Med. 1976; 59:637–647. [PubMed: 967136]
3. Pomerance A. Ballooning Deformity (Mucoid Degeneration) of Atrioventricular Valves. Br Hear J. 1969; 31:343–351.
4. Avierinos J, Gersh BJ, Melton JI, Bailey KR, Shub C, Nishimura RA, et al. Natural History of Asymptomatic Mitral Valve Prolapse in the Community. Circulation. 2002; 106:1355–1361. [PubMed: 12221052]
5. Suri RM, Schaff HV, Dearani Ja, Sundt TM, Daly RC, Mullany CJ, et al. Survival advantage and improved durability of mitral repair for leaflet prolapse subsets in the current era. Ann Thorac Surg. 2006; 82:819–826. [PubMed: 16928491]
6. Suri RM, Burkhart HM, Daly RC, Dearani JA, Park SJ, Sundt TM, et al. Robotic mitral valve repair for all prolapse subsets using techniques identical to open valvuloplasty: Establishing the benchmark against which percutaneous interventions should be judged. J Thorac Cardiovasc Surg. 2011; 142:970–979. [PubMed: 21911231]
7. Chitwood WR, Rodriguez E, Chu MW, Hassan A, Ferguson TB, Vos PW, et al. Robotic mitral valve repairs in 300 patients: a single-center experience. J Thorac Cardiovasc Surg. 2008; 136:436–441. [PubMed: 18692654]
8. Enriquez-Sarano M, Avierinos J-F, Messika-Zeitoun D, Detaint D, Capps M, Nkomo V, et al. Quantitative determinants of the outcome of asymptomatic mitral regurgitation. N Engl J Med. 2005; 352:875–883. [PubMed: 15745978]
9. Ng CM, Cheng A, Myers LA, Martinez-Murillo F, Jie C, Bedja D, et al. TGF-β dependent pathogenesis of mitral valve prolapse in a mouse model of Marfan syndrome. J Clin Invest. 2004; 114:1586–1592. [PubMed: 15546004]
10. Aupperle H, März I, Thielebein J, Kiefer B, Kappe A, Schoon H. Immunohistochemical characterization of the extracellular matrix in normal mitral valves and in chronic valve disease (endocardiosis) in dogs. Res Vet Sci. 2009; 87:277–283. [PubMed: 19246062]
11. Geirsson A, Singh M, Ali R, Abbas H, Li W, Sanchez JA, et al. Modulation of Transforming Growth Factor-β Signaling and Extracellular Matrix Production in Myxomatous Mitral Valves by Angiotensin II Receptor Blockers. Circulation. 2012; 126:189–197. [PubMed: 22665718]
12. Hagler MA, Hadley TM, Zhang H, Mehra K, Roos CM, Schaff HV, et al. TGF-β signalling and reactive oxygen species drive fibrosis and matrix remodelling in myxomatous mitral valves. Cardiovasc Res. 2013; 99:175–184. [PubMed: 23554457]
13. Rabkin E, Aikawa M, Stone JR, Fukumoto Y, Libby P, Schoen FJ. Activated Interstitial Myofibroblasts Express Catabolic Enzymes and Mediate Matrix Remodeling in Myxomatous Heart Valves. Circulation. 2001; 104:2525–2532. [PubMed: 11714645]
14. Singh RG, Cappucci R, Kramer-fox R, Roman MJ, Kligfield P, Borer JS, et al. Severe Mitral Regurgitation Due to Mitral Valve Prolapse: Risk Factors for Development, Progression, and Need for Mitral Valve Surgery. Am J Cardiol. 2000; 85:193–198. [PubMed: 10955376]
15. Farkas IJ, Szántó-Várnagy A, Korcsmáros T. Linking proteins to signaling pathways for experiment design and evaluation. PLoS One. 2012; 7:e36202. [PubMed: 22558382]

16. Hocevar BA, Smine A, Xu X, Howe PH. The adaptor molecule Disabled-2 links the transforming growth factor β receptors to the Smad pathway. EMBO J. 2001; 20:2789–2801. [PubMed: 11387212]
17. Onichtchouk D, Chen Y-G, Dosch R, Gawantka V, Delius H, Massague J, et al. Silencing of TGF-β signalling by the pseudoreceptor BAMBI. Nature. 1999; 40:480–485. [PubMed: 10519551]
18. Vanlandewijck M, Raja E, Kowanetz M, Watanabe Y, Kowanetz K, Vasilaki E, et al. Transcriptional Induction of Salt-inducible Kinase 1 by Transforming Growth Factor β Leads to Negative Regulation of Type I Receptor Signaling in Cooperation with the Smurf2 Ubiquitin Ligase. J Biol Chem. 2012; 287:12867–12878. [PubMed: 22378783]
19. Feng X, Liang Y, Liang M, Zhai W, Lin X. Direct Interaction of c-Myc with Smad2 and Smad3 to Inhibit TGF-β-Mediated Induction of the CDK Inhibitor p15 Ink4B. Mol Cell. 2002; 9:133–143. [PubMed: 11804592]
20. Wotton D, Lo RS, Lee S. A Smad Transcriptional Corepressor. Cell. 1999; 97:29–39. [PubMed: 10199400]
21. Miller JD, Weiss RM, Heistad DD. Calcific Aortic Valve Stenosis : Methods, Models, and Mechanisms. Circ Res. 2012; 108:1392–1412. [PubMed: 21617136]
22. Sainger R, Grau JB, Branchetti E, Poggio P, Seefried WF, Field BC, et al. Human Myxomatous Mitral Valve Prolapse: Role of Bone Morphogenetic Protein 4 in Valvular Interstitial Cell Activation. J Cell Physiol. 2011; 227:2595–2604. [PubMed: 22105615]
23. Tamai K, Semenov M, Kato Y, Spokony R, Liu C, Katsuyama Y, et al. LDL-receptor-related proteins in Wnt signal transduction. Nature. 2000; 407:530–535. [PubMed: 11029007]
24. Qiang Y, Barlogie B, Rudikoff S, Shaughnessy JD. Dkk1-induced inhibition of Wnt signaling in osteoblast differentiation is an underlying mechanism of bone loss in multiple myeloma. Bone. 2008; 42:669–680. [PubMed: 18294945]
25. Kim K, Wagle M, Tran K, Zhan X, Dixon MA, Liu S, et al. R-Spondin Family Members Regulate the Wnt Pathway by a Common Mechanism. Mol Biol Chem. 2008; 19:2588–2596.
26. Xu S, Gotlieb AI. Wnt3a/β-catenin increases proliferation in heart valve interstitial cells. Cardiovasc Pathol. 2013; 22:156–166. [PubMed: 22889676]
27. Van der Deen M, Akech J, Wang T, FitzGerald TJ, Altieri DC, Languino LR, et al. The cancer-related Runx2 protein enhances cell growth and responses to androgen and TGFbeta in prostate cancer cells. J Cell Biochem. 2010; 109:828–837. [PubMed: 20082326]
28. Baniwal SK, Little GH, Chimge N-O, Frenkel B. Runx2 controls a feed-forward loop between androgen and prolactin-induced protein (PIP) in stimulating T47D cell proliferation. J Cell Physiol. 2012; 227:2276–2282. [PubMed: 21809344]
29. Akech J, Wixted JJ, Bedard K, van der Deen M, Hussain S, Guise Ta, et al. Runx2 association with progression of prostate cancer in patients: mechanisms mediating bone osteolysis and osteoblastic metastatic lesions. Oncogene. 2010; 29:811–821. [PubMed: 19915614]
30. Caira FC, Stock SR, Gleason TG, McGee EC, Huang J, Bonow RO, et al. Human degenerative valve disease is associated with up-regulation of low-density lipoprotein receptor-related protein 5 receptor-mediated bone formation. J Am Coll Cardiol. 2006; 47:1707–1712. [PubMed: 16631011]
31. Angel CE, Lala A, Chen C-JJ, Edgar SG, Ostrovsky LL, Dunbar PR. CD14+ antigen-presenting cells in human dermis are less mature than their CD1a+ counterparts. Int Immunol. 2007; 19:1271–1279. [PubMed: 17804688]
32. Cao W, Lee SH, Lu J. CD83 is preformed inside monocytes, macrophages and dendritic cells, but it is only stably expressed on activated dendritic cells. Biochem J. 2005; 93:85–93. [PubMed: 15320871]
33. Ishida Y, Gao J, Murphy PM. Chemokine Receptor CX3CR1 Mediates Skin Wound Healing by Promoting Macrophage and Fibroblast Accumulation and Function. J Immunol. 2008; 180:569–579. [PubMed: 18097059]
34. Liu AC, Joag VR, Gotlieb AI. The Emerging Role of Valve Interstitial Cell Phenotypes in Regulating Heart Valve Pathobiology. Am J Pathol. 2007; 171:1407–1418. [PubMed: 17823281]
35. Akhmetshina A, Palumbo K, Dees C, Bergmann C, Venalis P, Zerr P, et al. Activation of canonical Wnt signalling is required for TGF-β-mediated fibrosis. Nat Commun. 2012; 3:1–12.

36. Lee K, Kim H, Li Q, Chi X, Ueta C, Komori T, et al. Runx2 Is a Common Target of Transforming Growth Factor-β1 and Bone Morphogenetic Protein 2, and Cooperation between Runx2 and Smad5 Induces Osteoblast-Specific Gene Expression in the Pluripotent Mesenchymal Precursor Cell Line C2C12. Mol Cell Biol. 2000; 20:8783–8792. [PubMed: 11073979]

37. Gray MO, Long CS, Kalinyak JE, Li HT, Karliner JS. Angiotensin II stimulates cardiac myocyte hypertrophy via paracrine release of TGF-β1 and endothelin-1 from fibroblasts. Cardiovasc Res. 1998; 40:352–363. [PubMed: 9893729]

38. Fujisaka T, Hoshiga M, Hotchi J, Takeda Y, Jin D, Takai S, et al. Angiotensin II promotes aortic valve thickening independent of elevated blood pressure in apolipoprotein-E deficient mice. Atherosclerosis. 2013; 226:82–87. [PubMed: 23177972]

39. Tokuda K, Kai H, Kuwahara F, Yasukawa H, Tahara N, Kudo H, et al. Pressure-independent effects of angiotensin II on hypertensive myocardial fibrosis. Hypertension. 2004; 43:499–503. [PubMed: 14699000]

40. Cassis LA, Gupte M, Thayer S, Zhang X, Charnigo R, Howatt Da, et al. ANG II infusion promotes abdominal aortic aneurysms independent of increased blood pressure in hypercholesterolemic mice. Am J Physiol Hear Circ Physiol. 2009; 296:H1660–1665.

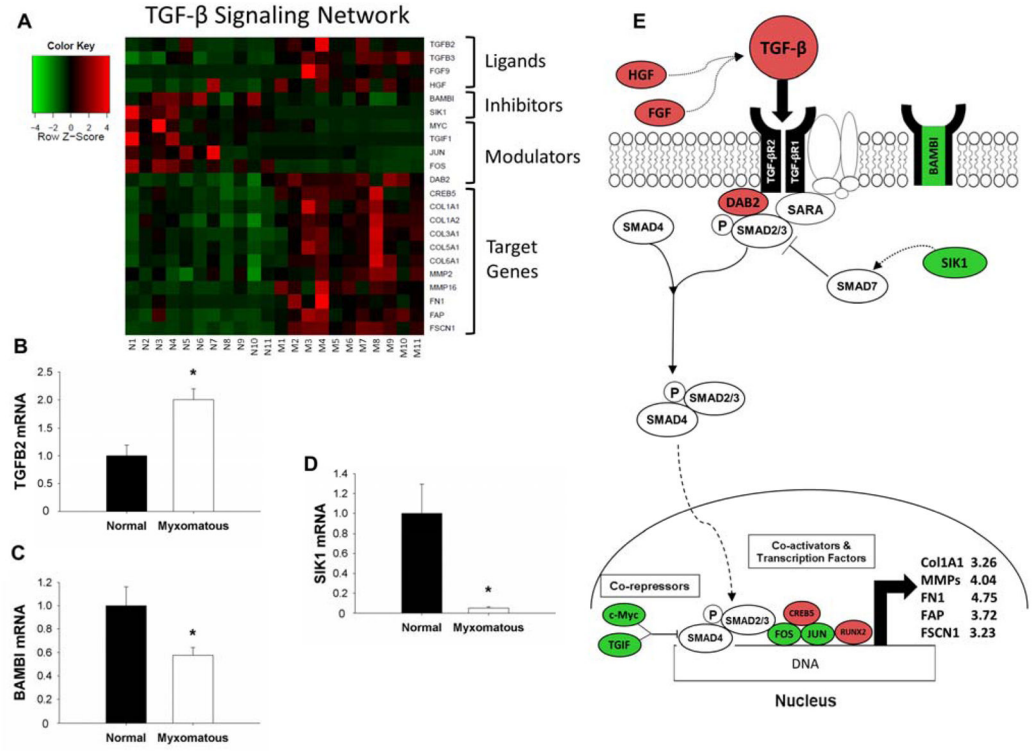

Figure 1. Changes in Transforming Growth Factor-β (TGF-β) signaling in myxomatous mitral valve tissue

A) Heat map of differentially expressed canonical TGF-β signaling-related genes in myxomatous (columns M1–M11) versus non-myxomatous (columns N1–N11) human mitral valves. Red = increased expression, and green = reduced expression. B–D) qRT-PCR confirmation of changes in TGF-β2 ligand (B), BAMBI (C) and SIK1 (D) expression in myxomatous versus non-myxomatous mitral valve tissue (n=11 non-myxomatous valves, n=10 myxomatous valves; * = $p<0.05$). qRT-PCR experiments were performed on the same samples of human mitral valve tissue used for microarray analyses. E) For ease of reference, a simplified working model of alterations in TGF-β signaling in MMVD (color coding as for Panel 1A). For clarity, non-myxomatous control valves are referred to as “normal”. BAMBI = BMP and activin membrane-bound inhibitor homolog (Xenopus laevis); COL1A1 = Collagen, type I, alpha 1; COL1A2 = Collagen type I, alpha 2; COL3A1 = collagen type III, alpha 1; COL5A1 = Collagen type V, alpha 1; COL6A1 = Collagen type VI, alpha 1; CREB5 = Cycle AMP-responsive element-binding protein 5; DAB2 = Disabled homolog 2; FAP = Fibroblast activation protein; FGF9 = Fibroblast growth factor 9; FOS = FBJ murine osteosarcoma viral oncogene homolog; FN1 = Fibronectin 1; FSCN1 = Fascin 1; HGF = Hepatocyte growth factor; JUN = Jun proto-oncogene; MMP = Matrix metalloproteinase; SARA = SMAD anchor for receptor activation; SIK1 = Salt-inducible kinase 1; TGF-β2 = transforming growth factor-beta; TGF-βR = transforming growth factor-beta receptor; TGIF1 = TGF-β-induced factor homeobox 1.

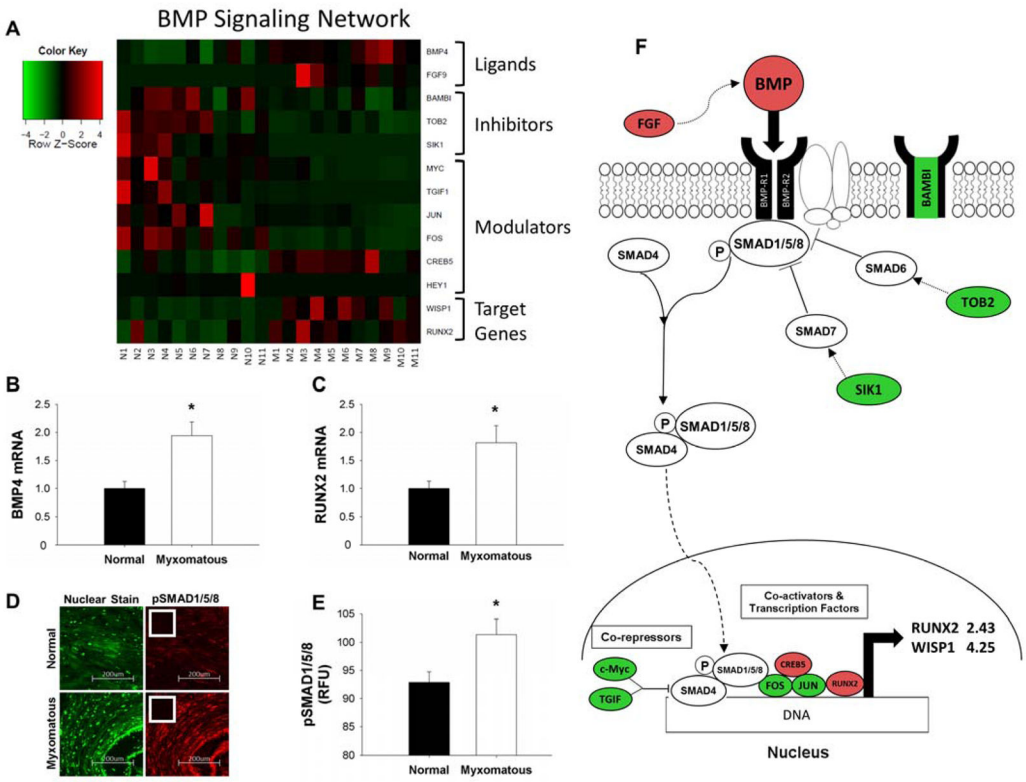

Figure 2. Alterations in Bone Morphogenetic Protein (BMP) signaling in myxomatous mitral valves

A) Heat map of differentially expressed canonical BMP signaling-related genes in myxomatous (columns M1–M11) versus non-myxomatous (columns N1–N11) human mitral valves. Red = increased expression, green = reduced expression. qRT-PCR confirmation of changes in BMP4 ligand (B) and Runx2 (C) expression in myxomatous versus non-myxomatous mitral valves (n=11 non-myxomatous valves, n=10 myxomatous valves; * = $p<0.05$). qRT-PCR experiments were performed on the same samples of human mitral valve tissue used for microarray analyses. D–E) Immunohistochemical staining (D) and subsequent quantitation (E) of pSMAD1/5/8 levels in myxomatous and non-myxomatous valves (20x magnification; inset negative control; n = 11 non-myxomatous valves, n = 11 mitral valves; $p < 0.05$). F) For ease of reference, a simplified working model of alterations in canonical BMP signaling in MMVD (color-coding as for Panel 2A). For clarity, non-myxomatous control valves are referred to as “normal”. BAMBI = BMP and activin membrane-bound inhibitor homolog (Xenopus laevis); BMP = Bone morphogenetic protein; BMP-R = Bone morphogenetic protein receptor; CREB5 = Cycle AMP-responsive element-binding protein 5; FGF9 = Fibroblast growth factor 9; FOS = FBJ murine osteosarcoma viral oncogene homolog; HEY1 = Hairy/enhancer-of-split related with YRPW motif 1; JUN = Jun proto-oncogene; RUNX2 = Runt-related transcription factor 2; SIK1 = Salt-inducible kinase 1; SMAD = SMA mothers against decapentaplegic; TGIF1= TGF-β-induced factor homeobox1 TOB2 = Transducer of ERBB2 2; WISP1 = Wnt-inducible signaling pathway protein 1.

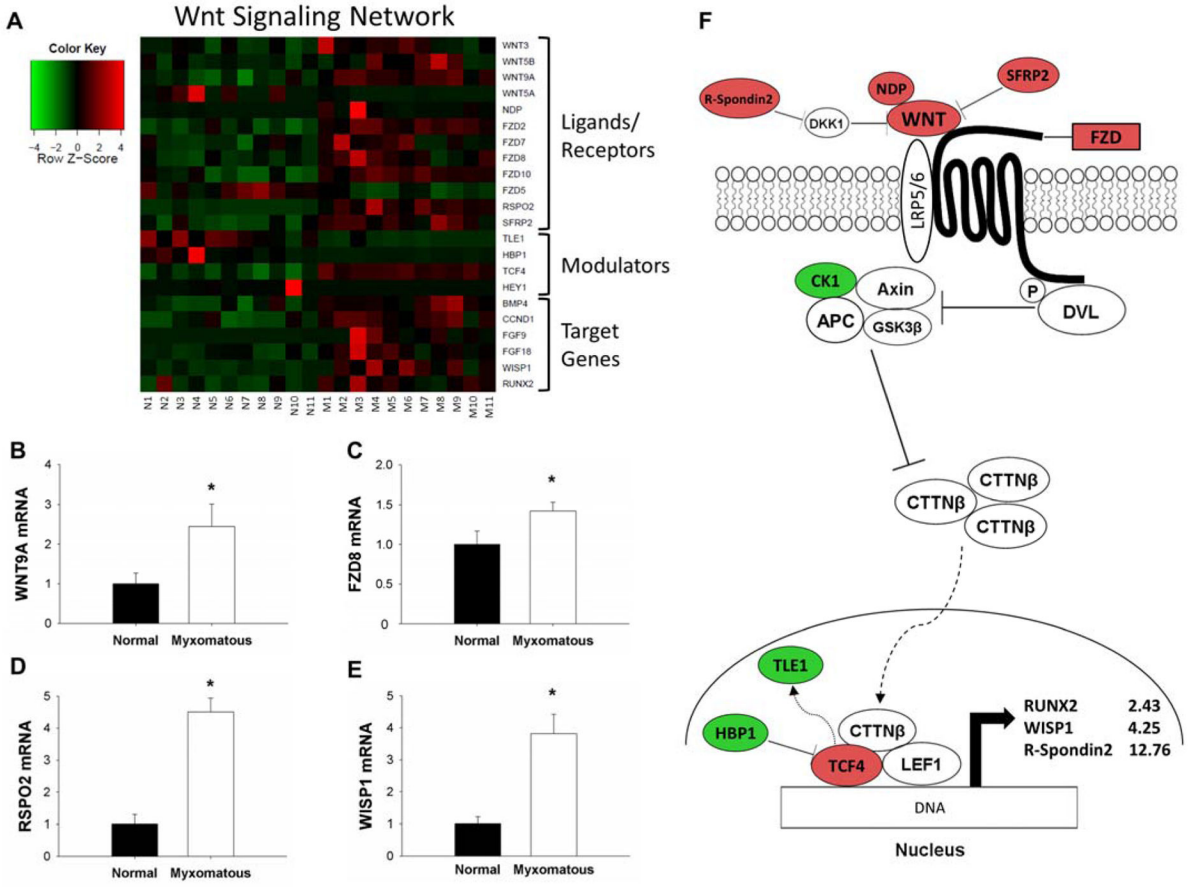

Figure 3. Changes in the Wnt/β-catenin signaling in MMVD

A) Heat map of differentially expressed canonical Wnt/β-catenin signaling-related genes in myxomatous (columns M1–M11) versus non-myxomatous (columns N1–N11) human mitral valves. Red = increased expression, green = reduced expression. B–E) qRT-PCR confirmation of differential gene expression of Wnt9a ligand (B), FZD8 receptor (C), R-spondin 2 (D) and WISP1 (E) in myxomatous versus non-myxomatous mitral valves (n = 11 non-myxomatous valves, n = 10 myxomatous valves;* = $p<0.05$). qRT-PCR experiments were performed on the same samples of human mitral valve tissue used for microarray analyses. F) For ease of reference, a simplified working model of canonical Wnt/β-catenin signaling in MMVD (color coding as for Panel 3A). For clarity, non-myxomatous control valves are referred to as “normal”. APC = Adenomatous polyposis coli; AXIN = Axis inhibition protein; BMP4 = bone morphogenetic protein 4; CK1 = Casein kinase 1, alpha 1; CTTNβ = Beta-catenin; DKK1 = Dickkopf 1 (Xenopus laevis); DVL = Dishevelled; FGF = fibroblast growth factor; FZD = Frizzled family receptor; HBP1 = HMG-box transcription factor 1; LEF1 = Lymphoid enhancer-binding factor 1; NDP = Norrie disease (pseudoglioma); RSPO2 = R-spondin 2; RUNX2 = Runt-related transcription factor 2; SFRP2 = Secreted frizzled-related protein 2; TCF4 = Transcription factor ; TLE1 = Transducin-like enhancer of split 1; WISP1 = Wnt-inducible signaling pathway protein 1; WNT = Wingless-type MMTV integration site family.

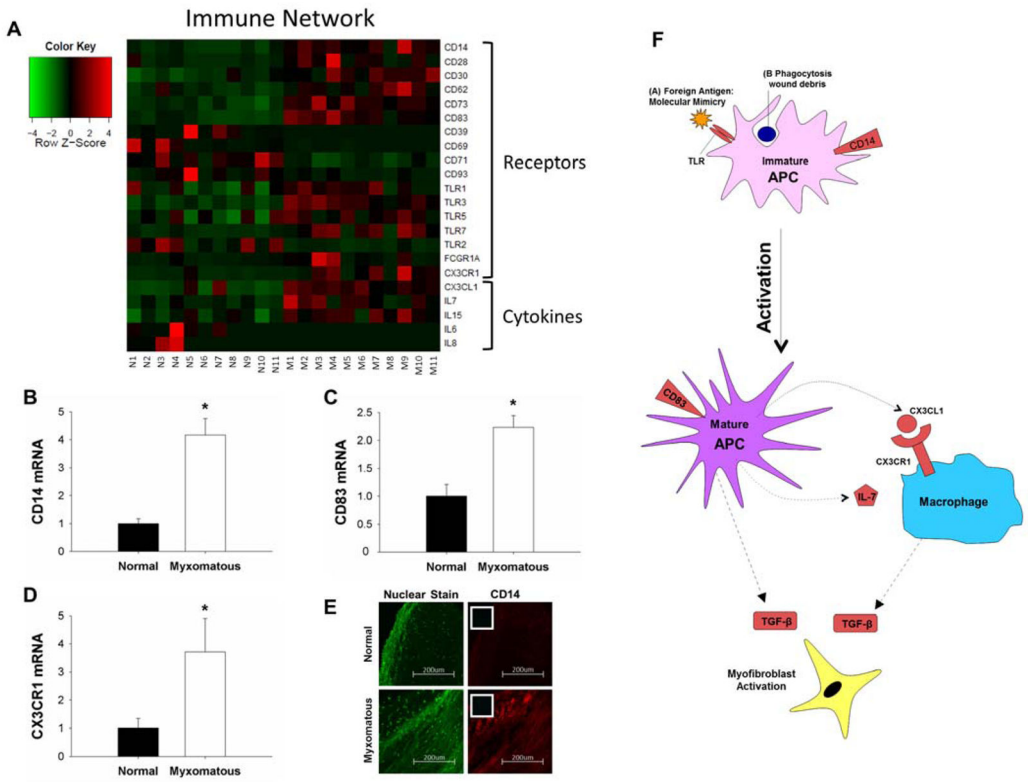

Figure 4. Changes in expression of immune cell markers and cytokines in MMVD

A) Heat map of differentially expressed genes associated with immune cell infiltration and inflammation in myxomatous (columns M1–M11) versus non-myxomatous (columns N1–N11) human mitral valves. Red = increased expression, green = reduced expression. B–D) Confirmation of changes in CD14 (B), CD83 (C), and CX3CR1 (D) gene expression in myxomatous versus non-myxomatous mitral valves (n = 11 non-myxomatous valves, n = 10 myxomatous valves; * = $p<0.05$). qRT-PCR experiments were performed on the same samples of human mitral valve tissue used for microarray analyses. E) Immunohistochemical staining for CD14 (20x magnification; inset negative control) in myxomatous and non-myxomatous mitral valve tissue (representative images from 11 non-myxomatous and 11 myxomatous mitral valves). F) For ease of reference, a simplified working model of potential interactions between immune cells and resident mitral valve interstitial cells in MMVD (color coding as for Panel 4A). For clarity, non-myxomatous control valves are referred to as “normal”. APC = Antigen presenting cell; CD = Cluster of differentiation; CX3CL1 = Chemokine (C-X3-C motif) ligand 1; CX3CR1 = Chemokine (C-X3-C motif) receptor 1; FCGR1A = Fc fragment of IgG high affinity Ia receptor; IL = Interleukin; TLR = Toll-like receptor.

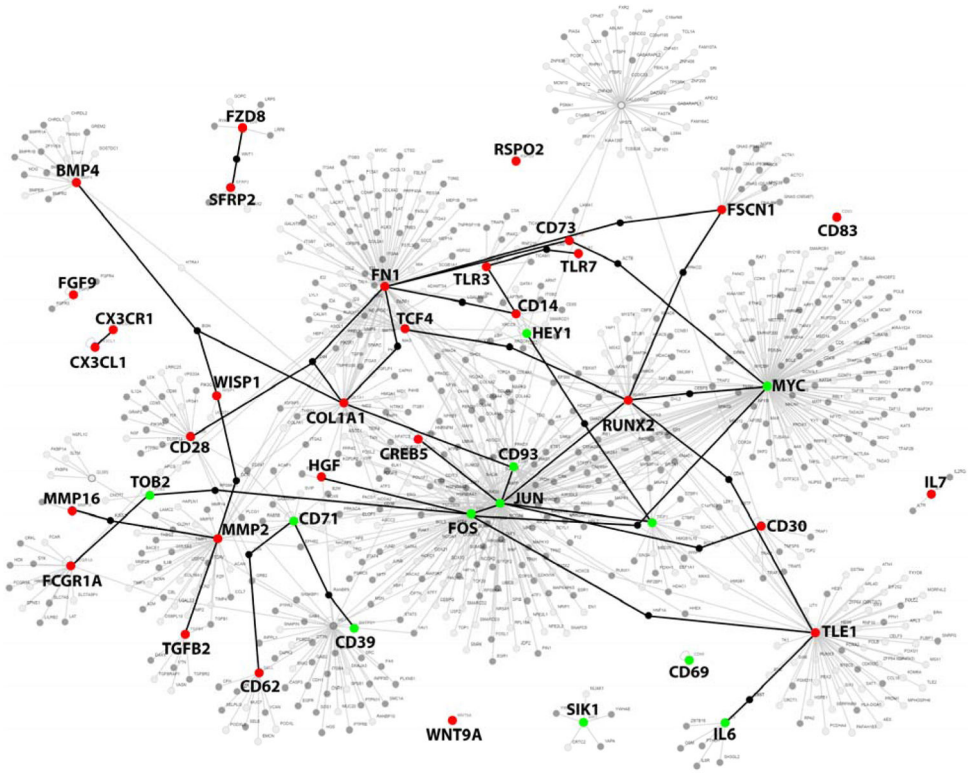

Figure 5. Potential molecular cross-talk between TGF-β, BMP, Wnt/β-catenin and Immune networks in MMVD

Highlighted nodes represent genes from all heatmaps in Figures 1–4 that were differentially expressed between myxomatous and non-myxomatous valves. Red denotes increased gene expression, green denotes reduced expression. Connections between nodes (i.e. edges) represent potential first-order interactions between 2 proteins. For clarity, genes used to induce the network are highlighted in capital text, and a subset of potential interactions is highlighted using bolded edges. BMP4, Bone morphogenetic protein; CD, cluster of differentiation; CDKN1A, Cyclin-dependent kinase 1A; COL1A1, Collagen, type I, alpha I; CREB5, Cycle AMP-responsive element-binding protein 5; CX3CL1, Chemokine (C-X3-C) motif ligand 1; CX3CR1, Chemokine (C-X3-C motif) receptor 1; DAB2, Disabled homolog 2; FGF9, fibroblast growth factor 9; FN1, fibronectin 1; FOS, FBJ murine osteosarcoma viral oncogene homolog; FSCN1, Fascin 1; FZD, Frizzled family receptor; HEY1, Hairy/enhancer-of-split related with YRPW motif 1; IL6, interleukin 6; IL7, interleukin 7; JUN, Jun proto-oncogene; MMP, matrix metalloproteinase; RUNX2, Runt-related transcription factor 2; SFRP2, Secreted frizzled-related protein 2; SIK1, salt-inducible kinase 1; TCF, Transcription factor; TGFB, Transforming growth factor-β; TLE1, Transducin-like enhancer of split 1; TLR, toll-like receptor; TOB2, Transducer of ERBB2; WISP1, Wnt-inducible signaling pathway protein 1.

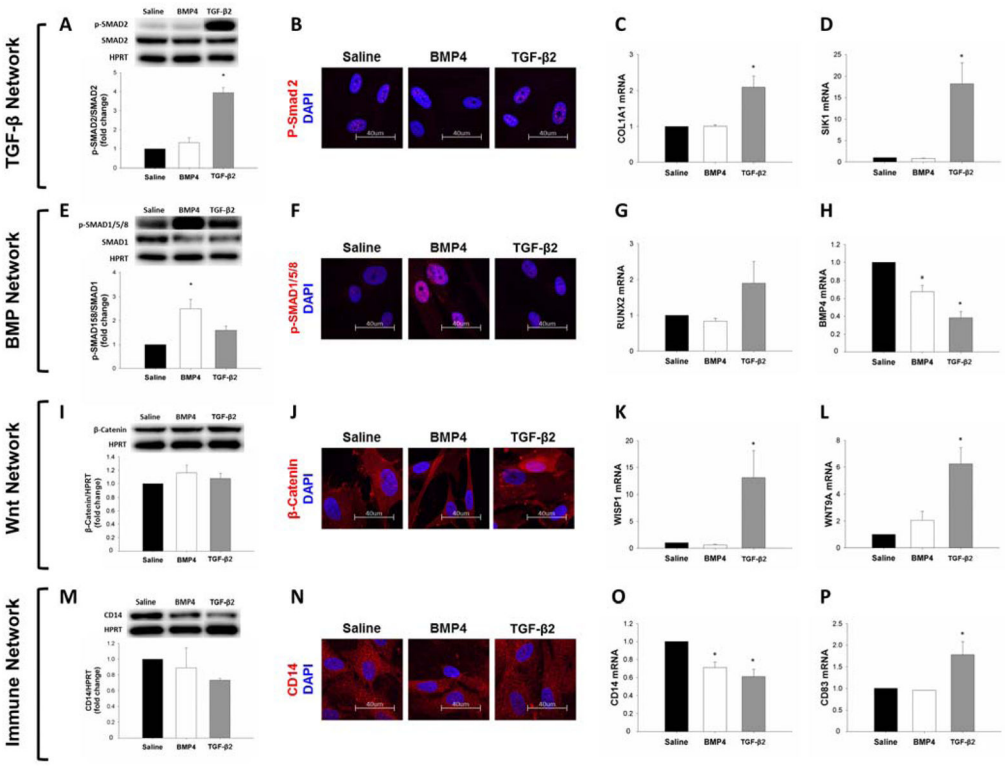

Figure 6. Effect of *in vitro* TGF-β and BMP4 treatment on TGF-β (A–D), BMP- (E–H), Wnt- (I–L) and immune signaling (M–P) in human mitral valve interstitial cells

pSMAD2 protein levels by western blot (A) were unchanged by BMP4 treatment but increased by TGF-β2 (24hr treatment). Immunocytochemistry (B) could not demonstrate a change in pSMAD2 with either treatment condition(100x magnification). COL1A1 (C) and SIK1 (D) gene expression levels in MVICs were not altered by BMP4 but increased by TGF-β2. pSMAD1/5/8 protein levels by western blot (E) and immunocytochemistry (100x magnification) (F) were increased by BMP4 treatment, but unaltered by TGF-β2 (24hr treatment). RUNX2 gene expression (G) by qRT-PCR was not changed by BMP4, but it tended to increase – though not significantly – following TGF-β2. BMP4 ligand levels (H) were markedly reduced by both treatments. Western blot analysis of total β-catenin protein (I) demonstrated no alteration following exogenous BMP4 or TGF-β2 (24hr treatment). Immunocytochemistry (100x magnification) (J) showed increased nuclear β-catenin with TGF-β2 but not BMP4 treatment. Gene expression of WISP1 (K) and Wnt9A (L) was unchanged by BMP4, but increased by TGF-β2. Protein levels of CD14 by western blot (M) and immunocytochemistry (100x magnification) (N) was not changed by BMP4 or TGF-β2 treatment (24hr treatment). Gene expression of CD14 by qRT-PCR (O) was reduced by both treatment conditions, while CD83 expression (P) though unaltered by BMP4 was increased by TGF-β2. BMP = Bone morphogenetic protein; CD = Cluster of differentiation; COL1A1 = collagen, type I, alpha I; Runx2 = Runt-related transcription factor 2; SIK1 = Salt-inducible kinase 1; SMAD = SMA mothers against decapentaplegic; TGF-β = Transforming growth factor-β; WISP1 = Wnt-inducible signaling pathway protein 1; Wnt9A = Wingless-type MMTV integration site family.

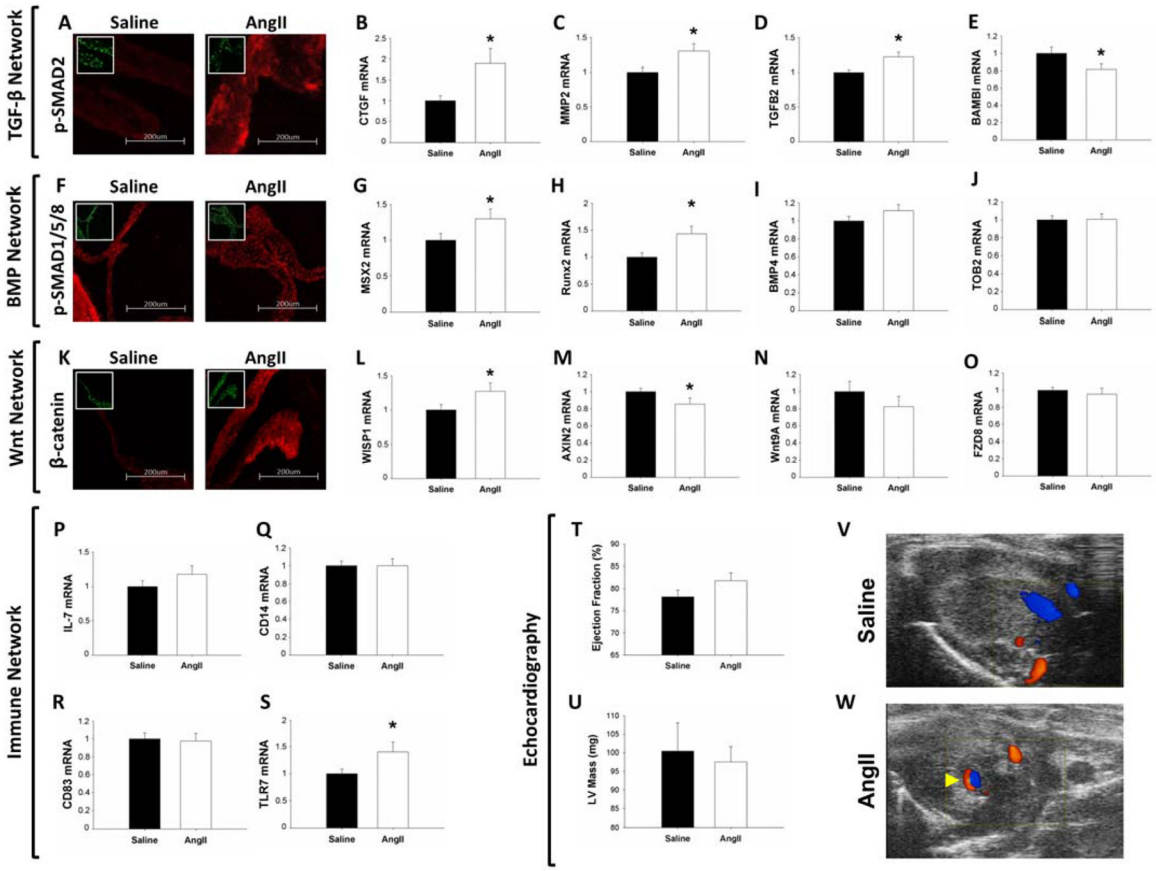

Figure 7. Molecular and phenotypic consequences of *in vivo* AngII infusion on murine mitral valves

A–E) Impact of AngII infusion on TGF-β signaling. Immunofluorescence of pSMAD2 (100x magnification; inset DAPI nuclear stain) (A) was enhanced in AngII treated mice. Expression of CTGF (B) and MMP2 (C), and TGF-β2 (D) was increased following AngII infusion, whereas expression of BAMBI (E) was reduced. F–J) Changes in BMP signaling following AngII treatment. Immunofluorescence of pSMAD1/5/8 (20x magnification; inset DAPI nuclear stain) (F) was unaltered by AngII infusion. mRNA levels of MSX2 (G) and Runx2 (H) were increased by AngII treatment, but expression of BMP4 (I) and TOB2 (J) was unchanged. K–O) Effects of AngII infusion on Wnt/β-catenin signaling in murine mitral valves. β-catenin immunofluorescence (20x magnification; inset DAPI nuclear stain) (K) was increased following AngII treatment. AngII increased expression of WISP1 (L) and decreased AXIN2 (M) expression. Wnt9A ligand (N) and FZD8 receptor (O) mRNA levels were unchanged by AngII infusion. P–S) Effect of AngII treatment on immune-network activation. Expression of interleukin 7 (P), CD14 (Q) and CD83 (R) was unchanged by AngII, whereas TLR7 levels (S) were increased. T–W) Echocardiographic evaluation of mitral valve and LV function in murine mitral valves. AngII infusion did not alter ejection fraction (T) or LV mass (U) in mice. V–W) Representative modified 2-chamber views of a saline-infused mouse without mitral regurgitation (V) and an AngII-infused mouse with trace mitral regurgitation (arrow) (W). (qRT-PCR: n=15 Saline vs n=13 AngII; IHC: n=8 Saline vs. n=8 AngII; * = $p<0.05$). AngII = Angiotensin II; AXIN2 = Axis inhibition protein

2; BAMBI = BMP and activin membrane-bound inhibitor homolog (Xenopus laevis); BMP = Bone morphogenetic protein; CD = cluster of differentiation; CTGF = Connective tissue growth factor; FZD8 = Frizzled family receptor 8; IL-7 = Interleukin 7; LV = Left ventricular; MMP2 = Matrix metalloproteinase 2; RUNX2 = Runt-related transcription factor 2; SMAD = SMA mothers against decapentaplegic; TGF-β = Transforming growth factor-β; TLR7 = Toll-like receptor 7; TOB2 = Transducer of ERBB2; WISP1; Wnt-inducible signaling pathway protein 1; Wnt9A = Wingless-type MMTV integration site family.